CONF-9308136--8

DESIGN FEATURES OF A HIGH-INTENSITY, CESIUM-SPUTTER/PLASMA-SPUTTER NEGATIVE ION SOURCE

G. D. Alton, G. D. Mills, and J. Dellwo†

Oak Ridge National Laboratory*

P. O. Box 2008

Oak Ridge, Tennessee 37831-6368

A versatile, high-intensity, negative ion source has been designed and is now under construction which can be operated in either the cesium-sputter or plasma-sputter mode. The cesium-sputter mode can be effected by installation of a newly designed conical-geometry cesium-surface ionizer; for operation in the plasma-sputter mode, the surface ionizer is removed and either a hot-filament or RF antenna plasma-discharge igniter is installed. A multicusp magnetic field is specifically provided confining the plasma in the radial direction when the plasma-sputter mode is selected. This arrangement allows comparison of the two modes of operation. Brief descriptions of the design features, ion optics, and anticipated performances of the two source geometries will be presented in this report.

†ORNL and Joint Institute for Heavy Ion Research, Oak Ridge, Tennessee.
*Managed by Martin Marietta Energy Systems, Inc., under contract No. DE-AC05-84OR21400 with the U.S. Department of Energy.

1. INTRODUCTION

As has been the case historically, ion source development continues to be driven by the needs of the basic and applied research communities and in more recent years, by the needs of the industrial communities for sources with improved performance attributes, including operational reliability, lifetime, beam quality (emittance), and intensity for an ever-increasing number of applications. To a large extent, the rapid advancement of negative ion source technology is attributable to the discovery of the technique of enhancing secondary negative ion sputter yields by covering the sample surface containing the material of interest with less than a monolayer of group IA elements [1]. A number of negative ion sources based on the sputter principle have been developed, several of which are described in the review paper of Ref. 2. All sources based on the sputter principle use group IA adsorbates (usually cesium) to enhance the probability for negative ion formation. The sputter technique has been used as a practical means for the generation of negative ion beams for a number of years. In such sources, positive ion beams, usually formed by either direct surface ionization of a group IA element or in a heavy noble gas (Ar, Kr, or Xe) plasma discharge seeded with alkali metal vapor, are accelerated to energies between a few hundred eV and several keV where they sputter a sample containing the element of interest. The presence of a fractional layer of a highly electropositive adsorbate, such as cesium, on the surface is critically important for the enhancement of negative ion yields during the sputtering process. A fraction of the sputter ejected particles leave the adsorbate covered surface as negative ions and are accelerated through an extraction aperture in the source. Sources based on this principle are widely employed to provide a variety of atomic and molecular negative ion beams for use in a growing number of applications, such as accelerator-based atomic, nuclear, and applied research, ion implantation, isotope separation, and the important

analytical fields of secondary ion mass spectrometry (SIMS) and tandem mass spectrometry (TMS).

In this report, we describe a versatile negative ion source that can be operated either in the cesium-sputter or plasma-sputter modes. The cesium-sputter version uses a newly designed conical-geometry cesium-surface ionizer to form the cesium ion beam which is used to sputter the sample, while the plasma-sputter version extracts xenon and cesium ions from a plasma to uniformly sputter a spherical sector sample. Each of these source types will serve as a prototype for evaluation for potential use in generating radioactive ion beams (RIBs) at the Holifield Radioaction Ion Beam Facility (HRIBF) now under construction at the Oak Ridge National Laboratory [3]; details of the sources which will be evaluated "on-line" at the HRIBF are given in these proceedings [4]. The design features, positive and negative ion optics, and anticipated performances of these two source types are described in this report.

2.0 NEGATIVE ION BEAM GENERATION

The ion beam intensity capabilities of sputter-type negative ion sources depend on many factors, including the electron affinity E_A of the species of interest, the work function of the metal surface ϕ, the cesium sputter ratio S of the sample material , the positive ion beam intensity I^+, and the positive/negative ion optics of the particular electrode system. The work function of the surface ϕ, in turn, depends on the type and coverage σ of the adsorbate material, as well as the properties of the sample material (e.g., intrinsic work function ϕ_0, electron affinity E_A, and ionization potential I_p) [5]. The fundamental aspects of the negative ion beam process are discussed in Refs. 6 and 7. If we neglect influences of surface adsorbates on the sputter process during surface bombardment (the presence of surface adsorbates will affect, by some degree, the

sputtering of surface atoms), the negative ion intensity can be expressed in analytical form according to

$$I^- \cong S\, I^+ P_i \tag{1}$$

where P_i is the probability for negative ion formation during the sputter process. Scaled Sigmund theory [8,9] or experimental data, where available, can be used to provide accurate estimates of sputter ratios for cesium or xenon on the material of interest.

The probability for negative ion formation can, in principle, be estimated from Nørskov and Lundqvist theory [10]. In the prescription of Ref. 10, the probability for negative ion formation can be cast into a simple energy-dependent form given by

$$P^- (E_2, \theta) = \frac{2}{\pi} \exp\left[-\beta \sqrt{M}\, (\phi(\sigma) - E_A + V_i) / \sqrt{2E_2}\, \cos\theta\right], \tag{2}$$

where ϕ is the work function of the surface (ϕ depends on the relative adsorbate coverage σ), E_A is the electron affinity of the ejected particle of mass M and energy E_2, V_i is the image potential induced in the surface by the escaping ion, θ is the polar angle of the sputtered ion with respect to the surface normal, and β is a constant. In Eq. 1, $\sqrt{2E_2/M}\, \cos\theta = v_\perp$ is the component of the velocity of the escaping particle perpendicular to the metal surface. The mechanism for ion formation based on this theory is a velocity-dependent form of surface ionization.

3.0 MECHANICAL DESIGN FEATURES

Aside from the components necessary to effect positive ionization of the cesium vapor and details of the sputter sample assembly, the cesium-sputter and plasma-sputter

sources are identical in all other respects. However, because separate discussions will be made of each source, certain details of the commonly shared construction features will be repeated in this report. The cesium-sputter and plasma-sputter negative ion sources are displayed, respectively, in Figs. 1 and 2. The sources share a common vacuum housing, cesium oven, high-voltage insulators, and extraction electrode system and are, therefore, identical in principle to the sources described in Ref. 6, with the exception of the type of ionizer heater when the cesium-sputter mode of operation is selected; conversion from the cesium-sputter mode to the plasma-sputter mode can be accomplished in a few minutes. The source assembly is composed of four major independent assemblies: (1) the sputter probe vacuum airlock assembly; (2) the source unit itself to which is attached the sputter probe vacuum assembly, the cesium access and gas feed assemblies, ionizer heater assembly (cesium-sputter mode) or either coaxial LaB_6 cathode or RF antenna assemblies for plasma ignition (plasma-sputter mode); (3) a freon- or water-cooled, stainless-steel vacuum chamber onto which is attached the NdFeB magnets for radial direction plasma confinement, and (4) a ceramic-to-metal-bonded alumina (Al_2O_3) high-voltage insulator to which is attached the extraction electrode system. The sources are constructed primarily of stainless steel and use metal-to-ceramic bonded high-voltage insulators and low-voltage feedthroughs. Boron nitride insulators are used in positions where vapor or sputter deposits could lead to insulator degradation. Design emphasis has been placed on the ability to rapidly change the source itself and all degradable components. The cesium oven is mounted externally, permitting easy access for servicing while providing excellent thermal isolation between the ionization chamber and the oven itself. The main source sub-assembly is modular and can be quickly inserted or removed from the freon-cooled housing assembly by thumb screws in a matter of a few minutes during periods of required maintenance. An important design feature allows removal and replacement of the internally mounted boron-nitride insulator without major disassembly of the source.

Thus, insulators which have been contaminated during prolonged source operation can be quickly replaced without significant down time.

The ionization chamber houses the ion exit aperture (typically 3 mm in diameter), the ionizer heater and heater mount (cesium-sputter mode) or LaB_6 cathode or RF antenna (plasma-sputter mode), and the boron-nitride insulator which can be interchanged while the source is under argon.. The probe assembly consists of a stainless steel tube with diameters ϕ = 10 mm for the cesium-sputter and ϕ = 13 mm for the plasma-sputter negative ion source, to which is attached the sample of interest. The sample diameter for the plasma-sputter mode of operation can be scaled to a maximum diameter of 20 mm according to the intensity requirements of the user. The samples are cooled by continuous freon or water flow through concentric tube arrangements. The sputter samples can be inserted into and withdrawn from the source through the airlock valve which is sealed against atmospheric pressure by a conventional elastomer gasket. The vacuum interlock assembly is attached to an externally mounted ceramic-to-metal insulator which, in turn, is fastened to the back flange of the source. The insulator is used to isolate the probe-vacuum airlock assembly from the source body. The gas feed nozzle and oven nozzle assemblies are attached to the back flange by metal-to-metal vacuum flanges and are spring loaded against the plasma discharge chamber by convoluted, high-spring-tension bellows. The nozzle-to-plasma-discharge chamber interfaces are designed to prevent support gas or cesium leakage at the interface. The vacuum chamber is made of stainless steel and is freon or water cooled. The chamber is inserted within the high-voltage insulator. Small permanent magnets are used at the ion exit aperture to deflect electrons which are also generated and accelerated from the sample during the sputter process.

For the plasma-sputter mode of operation, two geometries of sputter samples will be used. In cases where malleable sheet-metal material containing the species of interest is readily available, samples ~1 mm in thickness will be pressed by means of a die fixture into a 13-mm-diameter spherical sector probe with radius of curvature $\rho \simeq 30$ mm for focusing the negative ion beam generated in the sputtering process through the exit aperture of the source. Samples which are brittle must be machined from solid materials. Composite sintered compounds or mixtures of compounds will be typically 3 mm in thickness with a spherical radius of 30 mm machined into the face of the material. These samples will be indirectly cooled by clamping the sample to a spherical or flat geometry copper heat sink appropriately contoured to the respective sample geometry. The sputter probe assembly will be cooled by a freon heat-exchange unit maintained at 15°C.

The vacuum chamber is equipped with freon or water coolant passages to protect the NdFeB plasma discharge confinement magnets from thermal degradation by the radiant power incident on the walls of the chamber arising from the plasma discharge. Plasma confinement is effected by the use of sixteen rows of NdFeB permanent magnets, equally spaced circumferentially around the diameter of the cylindrical plasma chamber. The polarities of the multicusp magnets alternate in sign to produce the well known multicusp magnetic field which is effective in confining the plasma in the radial direction. These magnets will not be removed whenever the source is operated in the cesium-sputter mode. The ion exit aperture is equipped with a set of dipole AlNiCo magnets to inhibit electron extraction from the source and thereby reduce loading to the extraction power supply. The source is attached to the vacuum chamber by means of thumb screws for ease in removal and installation for cleaning and other maintenance operations. The plasma-sputter source will use a RF antenna or a directly heated coaxial-geometry LaB_6 cathode to initiate and sustain the plasma discharge. The RF

antenna technique has previously been used in a high-intensity volume-type H^- source by Leung et al. [11] and recently by Tsuji and Ishikawa in an axial-geometry, plasma-sputter, negative-ion source [12].

4.0 THE CESIUM-SPUTTER NEGATIVE ION SOURCE

In cesium-sputter-type sources, the sample material is mounted on a negatively biased probe which is maintained at a potential difference with respect to the housing of 1-5 kV in a controlled flux of a neutral group IA element, usually cesium. In this source type, sputtering of the negatively biased sample material is effected by bombardment with positive cesium ions formed by direct-surface ionization of cesium which come in contact with a hot, high-work-function ionizer.

A number of cesium-sputter negative ion sources have been described in the literature (see, e.g., Refs. 2 and 6 for details of several cesium-sputter negative-ion sources). The sources differ only in the geometry of the ionizer, its spacing in relation to the negatively biased sample, the spacing of the sample in relation to the ion exit aperture, and the aperture size. Sources equipped with spherical- [13], ellipsoidal- [14], and cylindrical-geometry ionizers [15,16] have been developed at several laboratories. We describe the mechanical design features and ion optics of a source, quite similar to those described in Refs. 2 and 6, with the exception that the geometry of the cesium ionizer is conical. The cesium-sputter source is displayed in Fig. 1.

4.1 The Perveance of the Conical-Surface-Ionizer/Sputter Sample Electrode Configuration

The positive ion currents achievable in sources which use direct surface ionization for positive ion formation, such as the cesium-sputter negative ion source described below, can attain values up to the space charge limit of the particular electrode configuration. For such sources, the perveance K of the electrode configuration can be measured or computationally determined by solving Poisson's equation. The perveance K is defined by the following relationship between the positive ion current I^+ and the potential difference V between the sample and surface ionizer or plasma:

$$I^+ = KV^{3/2}. \tag{3}$$

The perveance is a function of the geometry of the electrode system or plasma/sputter probe interface and mass M of the bombarding ion species. Since we assume that the negative ion current increases in proportion to the positive ion current, the perveance K serves as a convenient measure for comparing ion sources. The perveances of several electrode configurations used in cesium-sputter negative ion sources are given in Ref. 6. Of course, the perveance in a plasma-sputter negative ion source depends on the plasma density, mass of the plasma species, and sputter sample potential relation to housing.

4.2 Ion Optics of the Cesium-Sputter Negative Ion Source

Positive ion optics. The geometrical configuration of the positive and negative ion generation regions of the source are readily amenable to simulation by solving Poisson's equation numerically for the chosen electrode system. The electron trajectory

computer code, described in Ref. 17, was used to determine the perveance of the electrode system and to calculate cesium ion trajectories in the presence of space charge through the electrode system. A conical-geometry ionizer with a 90° included angle was evaluated at a fixed axial location electrode configuration and then optimized by altering the position in a series of iterations until acceptable beam profiles were achieved for both the positive and negative ion beams. An example of positive cesium ion trajectories through the ionizer/sputter probe region of the source under space-charge-limited conditions is shown in Fig. 3; the perveance for the electrode system displayed in Fig. 3 was found to be $K = 4.3 \times 10^{-9}$ [$A/V^{3/2}$]. The computed ion current density resulting from positive ion impact at the sample surface is shown in Fig. 4. As noted, the positive ion current is distributed over a full diameter of ~6 mm. This feature is desirable for potential use for generating radioactive ion beams where good overlap between the condensed vapors and cesium ion beam is required; details of this particular application are discussed in Ref. 4 of these proceedings.

Negative ion optics. An example of the negative ion trajectories flowing counter-current to the positive ion beam through the electrode system is shown in Fig. 5. The negative ion beam current density at the sample surface is assumed to mimic that of the positive ion current density distribution shown in Fig. 4. The influence of the positive-ion beam space charge on the negative-ion beam is included in the simulations. The optics of this electrode system are favorable for conserving cesium because the aperture can be restricted appreciably over many other sources of this type.

5.0 THE PLASMA-SPUTTER NEGATIVE ION SOURCE

The original plasma-sputter negative ion source developments, described in Refs. 18-21, clearly demonstrated their abilities to generate high-intensity (several mA) pulsed

negative-ion beams of a wide spectrum of atomic and molecular species. In recent years, progress has also been made toward developing sources compatible with dc operation [22-24]. The pulsed-mode performance characteristics of this source type are particularly well suited for use in conjunction with the tandem electrostatic accelerator when used as an injector for heavy-ion synchrotron, while the dc mode of operation is commensurate with stand-alone tandem accelerator operation, as well as many other applications. For heavy-ion synchrotron injection applications, high-intensity, pulsed beams of widths 50-300 μs at repetition rates of 1-50 Hz for a wide spectrum of atomic and molecular species are typically required. However, the wide range of species and intensity capabilities of the source make it a viable candidate for a variety of other basic and applied research applications, including material surface modification, ion implantation, ion beam deposition, and isotope separation.

The intensity levels from the plasma-sputter, negative ion sources described in Refs. 18-23 are often higher by factors of 30-100 than those which can be generated in cesium sputter-type sources such as described in Ref. 6 and yet the emittances ε_n of beams provided by the source are comparable for pulsed-mode operation of these sources. The original plasma-sputter negative ion sources used rather large spherical-sector sputter cathodes made of the material of interest (~40 to 50 mm diameter). Of course, these source geometries can be scaled toward smaller cathodes at the expense of lower negative ion beam intensities, but improved emittance. Recently, Yurimato and Mori have developed a compact axial geometry plasma-sputter negative ion source with a 16-mm diameter cathode which operates in the dc mode [24]. The source has demonstrated beam intensities exceeding 1 mA of Cu^- with emittances at the 90% contour level of $\varepsilon_n \simeq 6\ \pi$ mm.mrad $(MeV)^{1/2}$ [25].

The plasma-sputter negative ion source, shown in Fig. 2, will operate in the dc mode and is expected to be capable of producing mA intensity levels of many species, including the chemically inert noble metals, such as Au^-, Pt^-, and Ir^-, which are difficult to generate in positive ion sources. The plasma will be ignited and sustained by use of a 1 kW RF power supply equipped with a pulsed-plasma igniter and automatic matching network. The ion beam intensities from the source are expected to be 66% of those observed from the source described in Ref. 24; as a consequence of the reduced sputter cathode diameter, the emittance will be lower, as well, ($\varepsilon_n \simeq 5\ \pi$ mm.mrad.$MeV^{1/2}$).

10.0 ION OPTICAL STUDIES

The advantage of the plasma-type sputter negative ion source lies in the fact that, when operated in a high-density plasma mode, the negatively biased sputter probe containing the material of interest is uniformly sputtered. This characteristic makes it possible to take advantage of the large area, spherical-geometry lens system which is formed between the spherical sector sputter probe and the plasma sheath which conforms to the geometry of the probe. Negative ions created in the sputter process are accelerated and focused through the plasma to a common focal point, usually chosen as the ion exit aperture of the source, and then pass into the field region of the extraction electrode system. Within the plasma, the ion beam is free of space charge effects. At high beam intensities, space charge effects come into play whenever the beam exits the plasma and enters the extraction region of the source. However, because the beam energy is 500-1000 eV upon exit from the plasma region of the source, space charge influences on the beam are reduced. After exiting the aperture, the beam is further accelerated to a final energy of 20 keV, typically.

The ion optics of the ion generation and extraction regions of the source are used as an essential aid in designing the source. An example of the negative ion optics of the source are shown in Fig. 6, which displays ion trajectories for a 1-mA Cu^- ion beam generated at the sputter probe surface and accelerated through the field-free region of the plasma where it exits into the extraction lens system and is further accelerated to a final energy of 20 keV. An intrinsic ion temperature of 10 eV was incorporated in the calculations; the particles were assumed to have an angular spread about the normal to the sample surface of $\pm 2°$.

References

1. V. E. Krohn, Jr., Appl. Phys. 38, 3523 (1962).
2. G. D. Alton, Nucl. Instr. and Meth. B73, 221 (1993).
3. The Oak Ridge Radioactive Ion Beam Facility, J. D. Garrett, G. D. Alton, C. Baktash, D. K. Olsen, and K. S. Toth, Nucl. Phys. A557, 7016 (1993).
4. G. D. Alton, D. L. Haynes, G. D. Mills, and D. K. Olsen, these proceedings.
5. G. D. Alton, Surf. Sci. 175, 226 (1986).
6. G. D. Alton, Nucl. Instr. and Meth. B37/38, 45 (1989).
7. G. D. Alton, Nucl. Instr. and Meth. B40/41, 302 (1989).
8. P. Sigmund, Phys. Rev. 184, 383 (1969).
9. G. D. Alton, D. H. Olive, M. L. Pinkham, and J. R. Olive, Rad. Effects and Defects in Solids 126, 331 (1993).
10. J. K. Nørskov and B. I. Lundqvist, Phys. Rev. B19, 5661 (1979).
11. K. N. Leung, G. J. DeVries, W. F. DiVergilio, R. W. Hamm, C. A. Hauck, W. B. Kunkel, D. S. McDonald, and M. D. Williams, Rev. Sci. Instr. 62, 100 (1990).
12. H. Tsuji and J. Ishikawa, Rev. Sci. Instr. 63, 2488 (1992).
13. G. D. Alton and G. D. Mills, IEEE Trans. Nucl. Sci. NS-32 (5), 1822 (1985).

14. G. D. Alton and J. W. McConnell, Nucl. Instr. and Meth. A268, 445 (1988)

15. R. Middleton, Nucl. Instr. and Meth. 214, 139 (1983).

16. G. D. Alton, Nucl. Instr. and Meth. A244, 133 (1986).

17. PBGUNS, Thunderbird Simulations, 626 Bradfield, Garland, Texas 75042-6005.

18. G. D. Alton, Y. Mori, A. Takagi,A. Ueno, and S. Fukumoto, Nucl. Instr. and Meth. A270, 194 (1988); Nucl. Instr. and Meth. B40/41, 1008 (1989).

19. Y. Mori, G. D. Alton, A. Takagi, A. Ueno, and S. Fukumoto, Nucl. Instr. and Meth. A273, 5 (1988).

20. G. D. Alton, Y. Mori, A. Takagi, A. Ueno, and S. Fukumoto, Rev. Sci. Instr. 61, 372 (1990).

21. G. D. Alton, Rev. Sci. Instr. 63, 2453 (1992).

22. Y. Mori and A. Takagi, Rev. Sci. Instr. 63, 2669 (1992)

23. H. Tsuji and J. Ishikawa, Rev. Sci. Instr. 63, 2488 (1992)

24. H. Yurimoto and Y. Mori, Rev. Sci. Instr. 64, 1146 (1993).

25. Y. Mori, Nucl. Instr. and Meth. A328, 146 (1993).

Figure Captions:

1. ORNL-DWG 93M-11405. Schematic drawing of the cesium-sputter, negative-ion source equipped with a conical-geometry, cesium-surface ionizer.
2. ORNL-DWG 93M-11406. Schematic drawing of the plasma-sputter, negative-ion source equipped with a RF antenna for plasma ignition and maintenance.
3. ORNL-DWG 93M-11407. Computational calculation of the positive-cesium-ion optics for space-charge-limited flow in the ionizer/sputter sample region. The perveance of the electrode system is $K = 4.3 \times 10^{-9}$ [$A/V^{3/2}$]; sputter sample potential: 2 keV; ion species: Cs^+.
4. ORNL-DWG 93M-11414. Computed cesium positive-ion beam current density distribution at the sample surface of the ion beam shown in Fig. 3.
5. ORNL-DWG 93M-11409. Computational simulation of the negative-ion optics in the region between the sample and the postacceleration electrode system. The influence of the positive ion beam space charge on the negative ion beam trajectories is included in the simulation. The negative-ion beam current density distribution at the sample surface is assumed to mimic that of the positive-ion current density distribution shown in Fig. 4, but at a lower beam intensity. Sputter sample voltage: 2 kV; species: Cu^-; ion beam intensity: 200 μA; final ion beam energy: 20 keV.
6. ORNL-DWG 93M-11408. Computational simulation of the negative-ion optics in the plasma-sputter, negative-ion source. The plasma is assumed to fully compensate space-charge effects during transit to the ion exit aperture; space-charge effects are then included after exit into the postacceleration field region. Sputter sample voltage: –500 kV; species: Cu^-; Ion beam intensity: 1 mA; final ion beam energy: 20 keV.

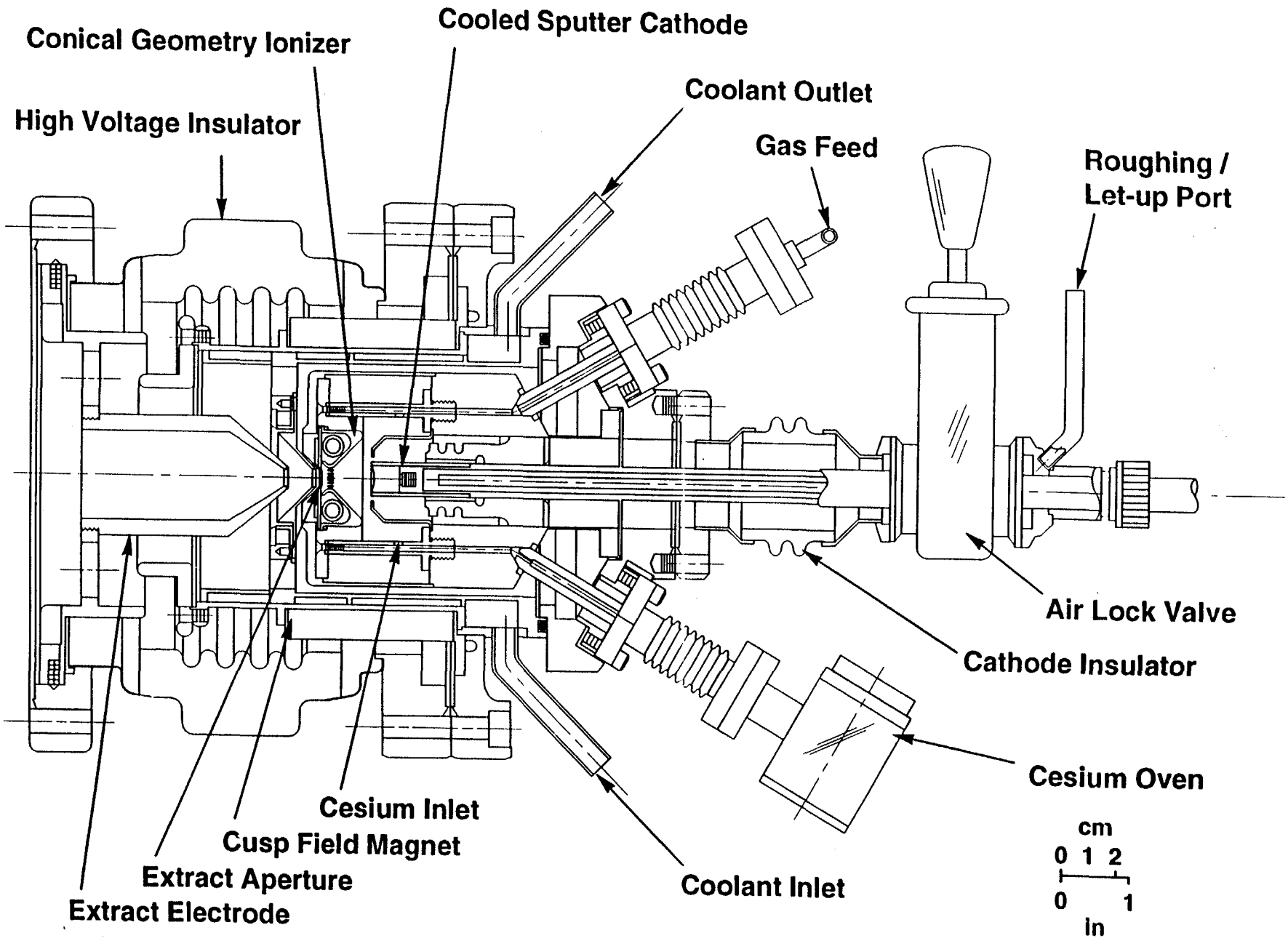
Conical Geometry Ionizer
Cooled Sputter Cathode
Coolant Outlet
High Voltage Insulator
Gas Feed
Roughing / Let-up Port
Air Lock Valve
Cathode Insulator
Cesium Oven
Cesium Inlet
Cusp Field Magnet
Extract Aperture
Extract Electrode
Coolant Inlet
cm
0 1 2
0 1
in

Figure 1

ORNL-DWG 93M-11406

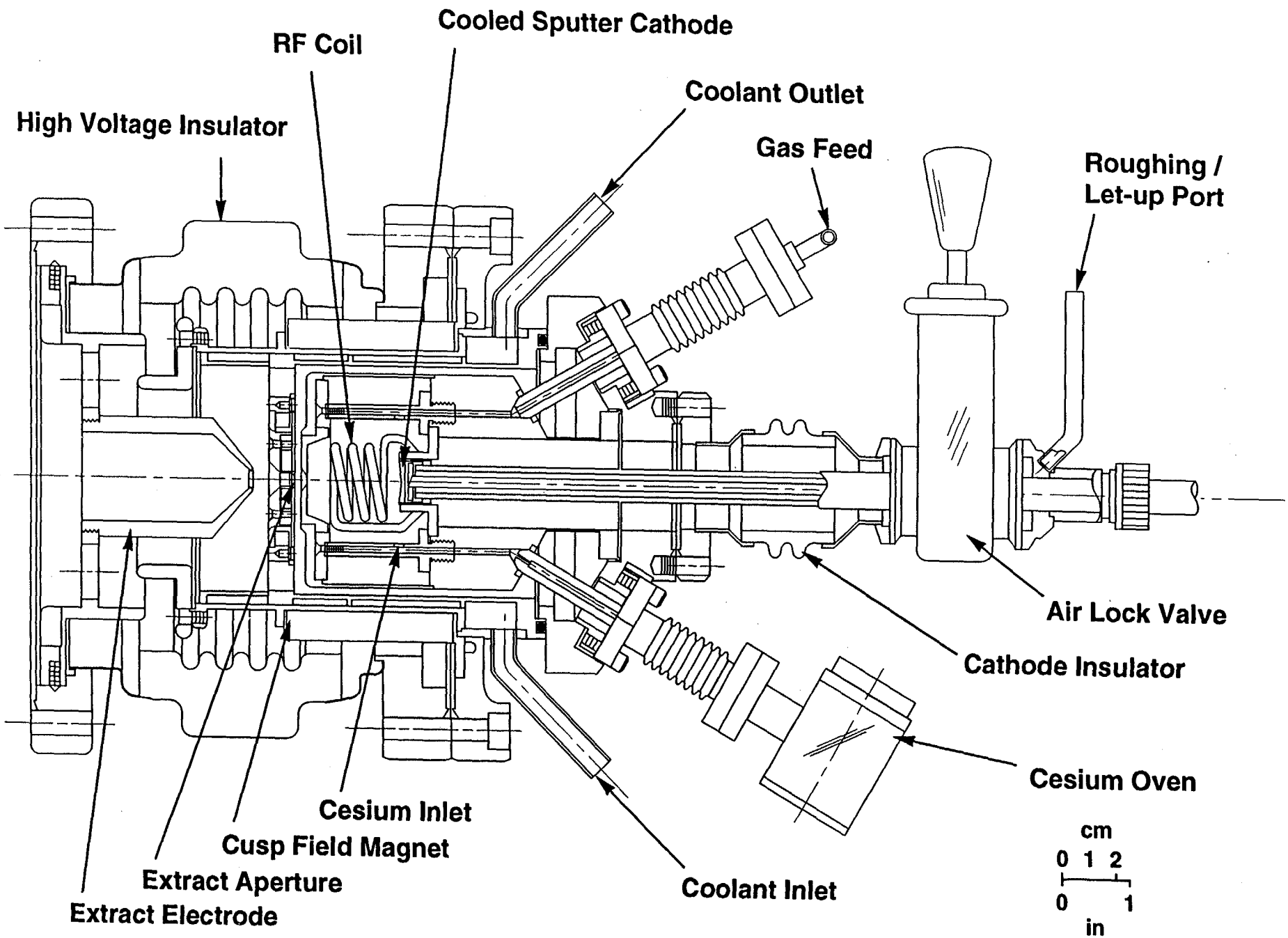

Figure 2

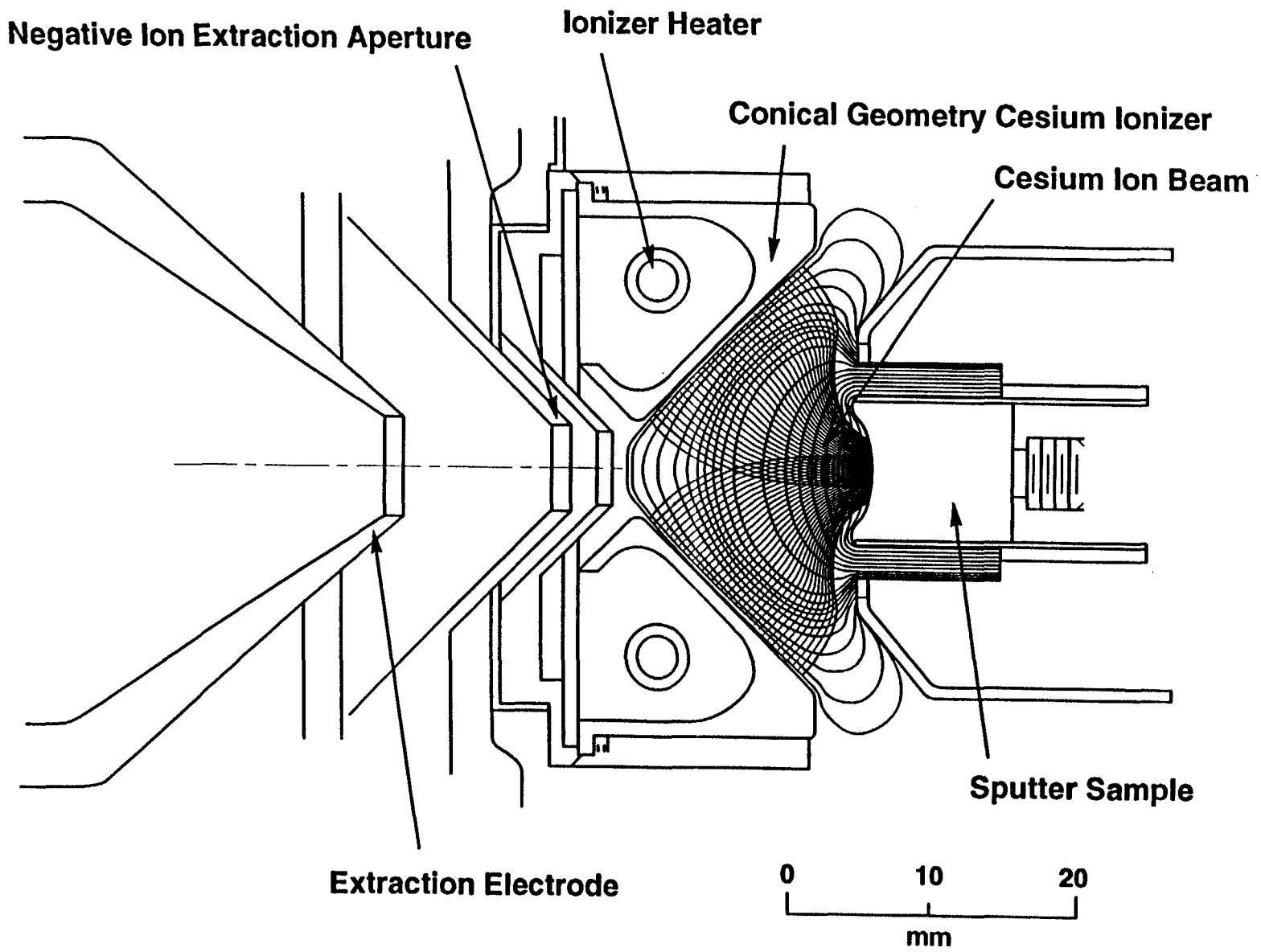
Negative Ion Extraction Aperture
Ionizer Heater
Conical Geometry Cesium Ionizer
Cesium Ion Beam
Sputter Sample
Extraction Electrode
0
10
20
mm

Figure 3

ORNL-DWG 93M-11414

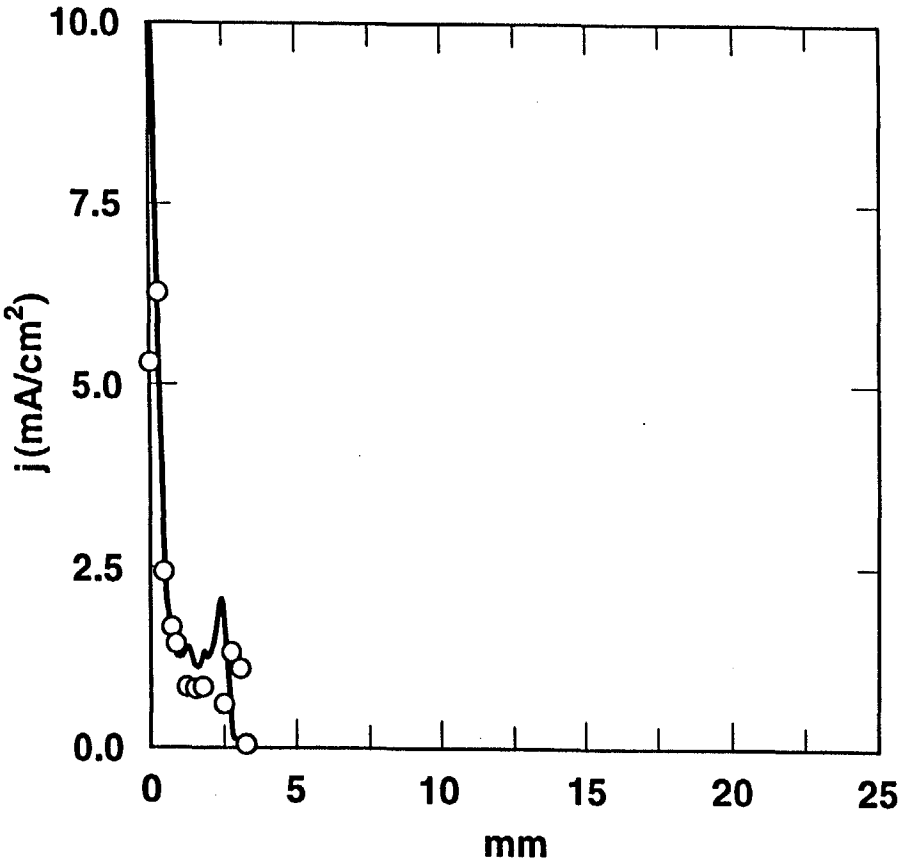

Figure 4

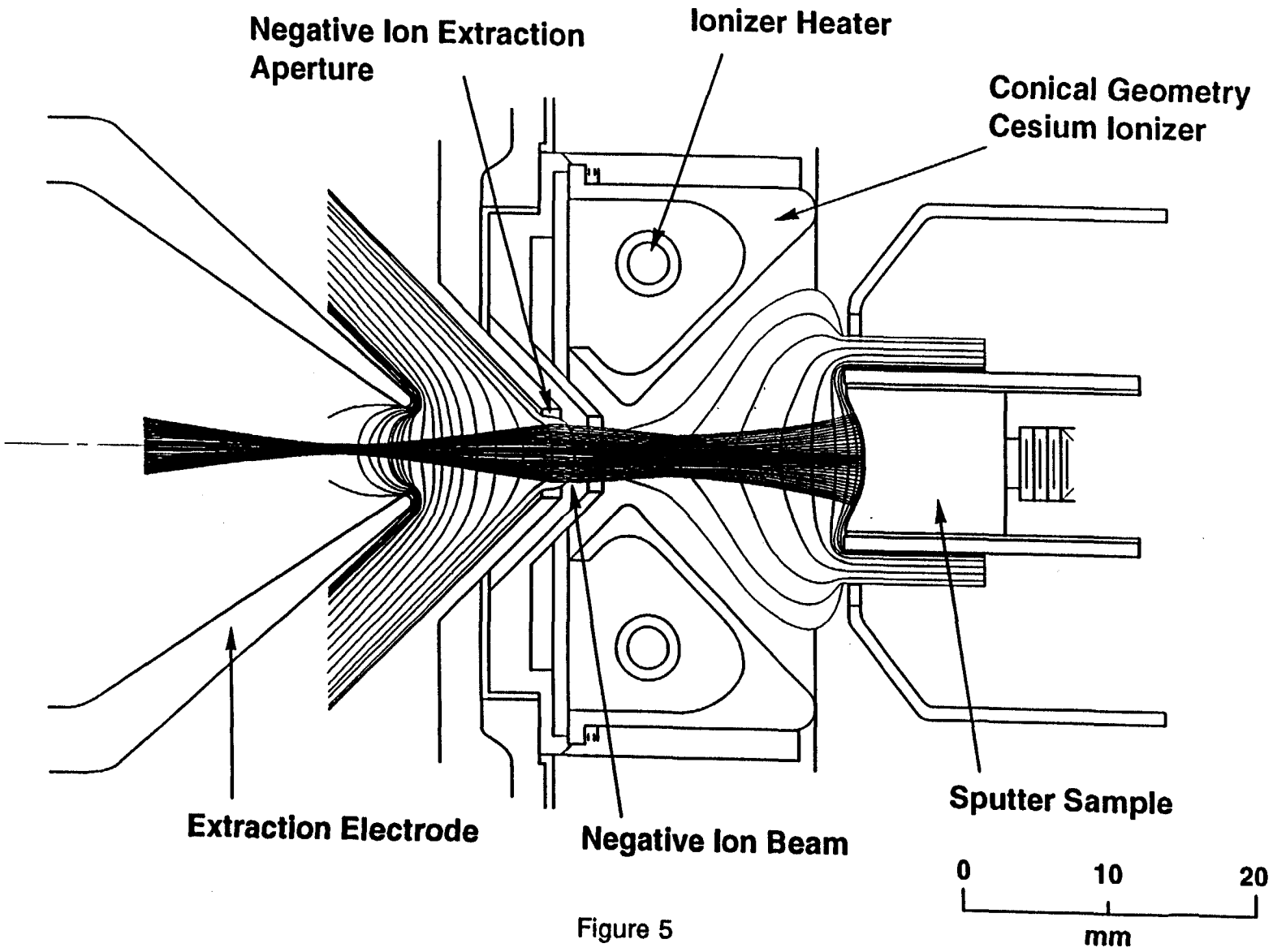
Negative Ion Extraction Aperture
Ionizer Heater
Conical Geometry Cesium Ionizer
Extraction Electrode
Negative Ion Beam
Sputter Sample
0
10
20
mm

Figure 5

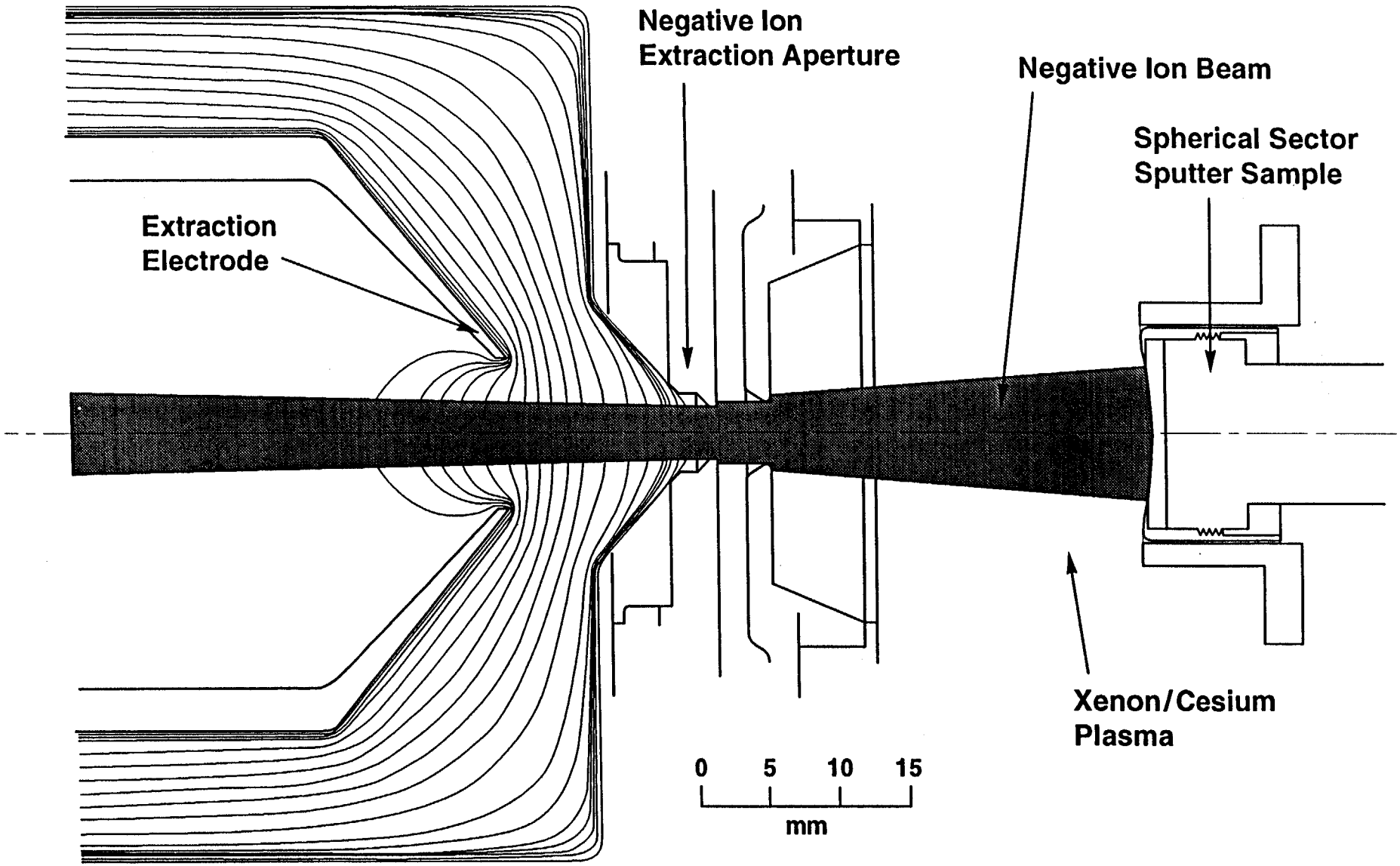
Negative Ion
Extraction Aperture
Negative Ion Beam
Spherical Sector
Sputter Sample
Extraction
Electrode
Xenon/Cesium
Plasma
0
5
10
15
mm

Figure 6